

InP-quantum dots in $\text{Al}_{0.20}\text{Ga}_{0.80}\text{InP}$ with different barrier configurations

Wolfgang-Michael Schulz, Robert Roßbach, Matthias Reischle, Gareth J. Beirne, Michael Jetter, and Peter Michler

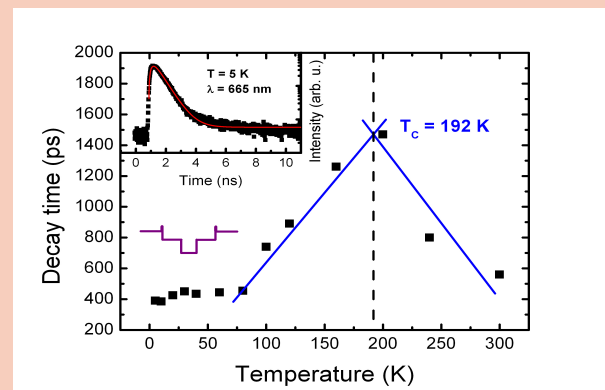
Institut für Halbleitertechnik und Funktionelle Grenzflächen, Allmandring 3, 70569 Stuttgart, Germany

Received XXXX, revised XXXX, accepted XXXX
Published online XXXX

PACS

* Corresponding author: e-mail: m.schulz@ihfg.uni-stuttgart.de, Phone: +49-711-685-69852, Fax +49-711-685-63866

Systematic ensemble photoluminescence studies have been performed on type-I InP-quantum dots in $\text{Al}_{0.20}\text{Ga}_{0.80}\text{InP}$ barriers, emitting at approximately 1.85 eV at 5 K. The influence of different barrier configurations as well as the incorporation of additional tunnel barriers on the optical properties has been investigated. The confinement energy between the dot barrier and the surrounding barrier layers, which is the sum of the band discontinuities for the valence and the conduction bands, was chosen to be approximately 190 meV by using $\text{Al}_{0.50}\text{Ga}_{0.50}\text{InP}$. In combination with 2 nm thick AlInP tunnel barriers, the internal quantum efficiency of these barrier configurations can be increased by up to a factor of 20 at elevated temperatures with respect to quantum dots without such layers.



Ensemble-transient (inset) and temperature dependent decay times of InP-QDs in $\text{Al}_{0.20}\text{GaInP}$ -barriers with surrounding $\text{Al}_{0.50}\text{GaInP}$ layers and AlInP tunnel barriers (sketch).

Copyright line will be provided by the publisher

1 Introduction Future quantum information applications with photonic devices requires high single-photon repetition rate emitters and detectors with high detection efficiencies. The highest sensitivity of a state-of-the-art avalanche-photodiode (APD) is nowadays in the red spectral range. These wavelengths are easily accessible by InP quantum dots (QDs) in (Al)GaInP-barriers. To make these emitters valuable for commercial applications, they should work at elevated temperatures. One possible solution is a deeper confinement potential for the QD to inhibit the thermal escape of the carriers. In our previous work we have shown that the maximum luminescence intensity can be reached for InP-QDs in $\text{Al}_{0.20}\text{Ga}_{0.80}\text{InP}$ -barriers especially at elevated temperatures [1]. The QD formation processes depend on the Al content of the barrier and thereby also strongly influence the optical properties of the QDs. In addition, the luminescence intensity temperature stability is strongly

enhanced by the increased confinement energy, which can be normally attributed to the energy difference between the QD emission energy and the barrier emission energy. To further increase the carrier confinement and thus the luminescence intensity temperature stability, the QDs were also embedded in different barrier layers (claddings). The investigation of different barrier configurations also provides a deeper insight into the electrical behavior of such structures when embedded in p-i-n-diode architectures for future light and laser applications, as the carrier injection (leakage current, threshold current,..) will depend on these layers.

2 Experimental procedure The self-assembled InP-QDs were grown by metal-organic vapor-phase epitaxy (MOVPE) with standard sources (trimethylgallium, trimethylindium, trimethylaluminum, arsine and phosphine) at low

Copyright line will be provided by the publisher

pressure (100 mbar) on (001) GaAs substrates oriented by 6° towards (111)A. The reference structure consists of a 100 nm GaAs buffer layer grown at 750°C and a 100 nm thick lattice matched $(\text{Al}_{0.20}\text{Ga}_{0.80})_{0.51}\text{In}_{0.49}\text{P}$ layer grown at 720°C . For the QD growth we deposited 2.1 monolayers (ML) of InP at a growth rate of 1.05 ML/s and a growth temperature of 650°C . The relatively low growth temperature was chosen in order to inhibit Al incorporation from the barrier into the QDs during their self-assembly [1]. Nevertheless, the absolute aluminum content in the dots is unknown. After a growth interruption of 20 s to ripen the QDs, a 30 nm cap-layer of $\text{Al}_{0.20}\text{Ga}_{0.80}\text{InP}$ followed in the case of samples for photoluminescence (PL) measurements. For the barrier configuration series the total sample-thickness (cap and barrier thickness) was kept constant. The QD active region consists of symmetric, 10 nm thick $\text{Al}_{0.20}\text{Ga}_{0.80}\text{InP}$ barriers. We kept the growth conditions of the active regions constant during the cladding series. $\text{Al}_{0.50}\text{Ga}_{0.50}\text{InP}$ cladding was used to fabricate both the abrupt and gradual interfaces. This gives an additional total band offset of $E_{\text{off}} = 190$ meV with respect to the barrier [2]. In addition to the integration of 2 nm thick tunnel barriers, the combination of an abrupt $\text{Al}_{0.50}\text{Ga}_{0.50}\text{InP}$ cladding with 2 nm thick AlInP tunnel barriers, providing an additional total band offset of 60 meV, was examined.

The samples were placed in a cold finger liquid He-flow cryostat to vary the ensemble PL measurement temperature. The samples were excited using frequency doubled Ti:sapphire-laser emission for both the time-resolved and time integrated PL. The luminescence was then dispersed using a 0.32 m Jobin-Yvon monochromator and detected by a multi-channel plate photomultiplier tube.

In order to perform micro-PL (μ -PL) experiments at 5 K, the samples were mounted in a liquid He-flow cryostat that can be scanned both horizontally and vertically using two stepper motors with an effective spatial resolution of 50 nm. The light to and from the QDs was transmitted through a $50\times$ microscope objective resulting in a laser spot diameter of approximately $1\ \mu\text{m}$ when focused accurately using a piezo-based actuator. The PL was dispersed using a 0.75 m spectrometer and detected by a liquid-nitrogen cooled charge-coupled device camera when taking spectra. For the photon statistics measurements, two single-photon counting avalanche photodiodes (APDs) were used, one in each path of a HanburyBrown and Twiss type setup realised using a 50/50 beamsplitter after the output of the monochromator [4, 5].

3 Results

3.1 Ensemble measurements The normalized spectra and sketches of their conduction-bandstructures for the samples with different barrier configurations are shown in Fig. 1. The lowest spectrum (a) in the graph corresponds to the reference. One can see, that the different configurations have almost no influence on the spectral position and the full width half maximum of the QD emission. The

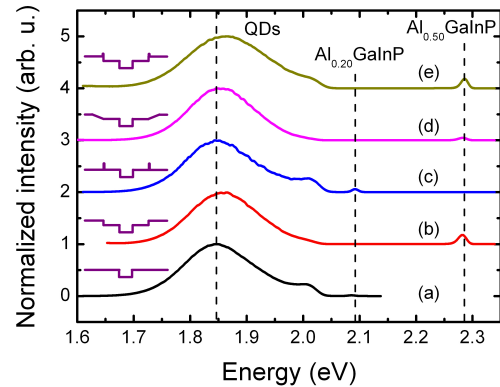


Figure 1 PL spectra of InP-QDs in $\text{Al}_{0.20}\text{GaInP}$ barriers with different barrier configurations, excited at 400 nm, $700\ \text{Wcm}^{-2}$ at 5 K. The growth and therefore the emission energy of the QDs, which is marked by the dashed vertical line at 1.847 eV, is not significantly influenced by the claddings. The other two vertical lines mark the emission of the $\text{Al}_{0.20}\text{GaInP}$ barrier at 2.09 eV and the $\text{Al}_{0.50}\text{GaInP}$ material at 2.28 eV. Emission from the AlInP tunnel barrier, which is expected at 2.33 eV, is not observed.

only change in the spectra (b), (d), (e) is the weak emission from the $\text{Al}_{0.50}\text{GaInP}$ observed at around 2.28 eV. Emission from the AlInP tunnel barrier is not observed. As the emission characteristics of QDs are strongly influenced by their size, we conclude that there is also no significant change in dot height and its distribution. Therefore the confinement energy E_C , which is the energetic difference between QD and barrier emission, remains almost constant at a value of approximately $E_C = 240$ meV. Fig. 2 shows an atomic force microscopy (AFM) height image of InP-QDs grown on an $\text{Al}_{0.20}\text{GaInP}$ barrier. The QDs exhibit an average height of around 4.3 nm, with a

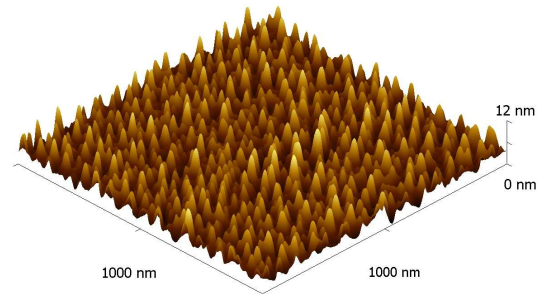


Figure 2 AFM height image of open (uncapped) InP-quantum dots on an $\text{Al}_{0.20}\text{GaInP}$ barrier (image size $1\times 1\ \mu\text{m}^2$). The average height is approximately 4.3 nm (zero error subtracted) and the diameter is approximately 30 nm.

sample surface density of approximately $5 \times 10^{10} \text{cm}^{-2}$. The major difference between the structures (insets) and the influence of the cladding on the emission characteristics can be seen in the temperature behavior of their relative intensities as depicted in Fig. 3. For comparison the tem-

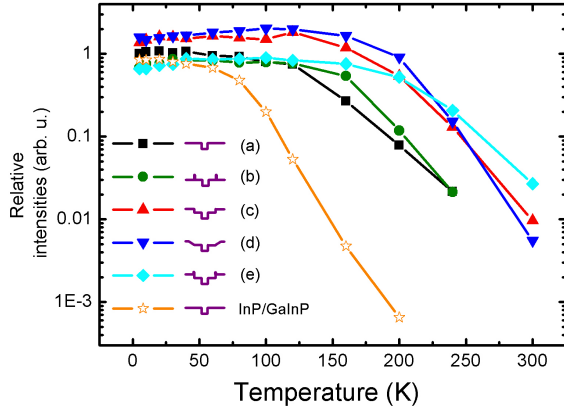


Figure 3 Temperature dependence of the relative intensities of InP-QDs in $\text{Al}_{0.20}\text{GaInP}$ barriers with different barrier configurations. For comparison the temperature dependence of InP-QDs in GaInP without cladding layers is also presented.

perature behavior for InP-QDs in GaInP without cladding (open stars) is also shown in this graph. At 200 K the InP-QDs in Al containing barriers show a PL intensity enhancement by more than a factor 100 with respect to QDs, emitting at the same energy, in GaInP. According to Fig. 3, the tunnel barriers (b) slightly reduce the intensity with respect to the reference structure (a). This is expected as they should reduce the number of excited carriers compared to the other cladding samples at comparable excitation powers. The highest intensity at low temperatures can be achieved using the graded barrier configuration (d), and is probably due to the associated gradient force that acts on the carriers. From a very basic point of view, this force F can be written as $\mathbf{F} = -q \cdot \nabla \Phi$, the gradient of the potential Φ (band offset between the barrier and the cladding) multiplied by the carrier charge q [3]. The carriers were pushed towards the QDs as this gradient force points in the direction of the local potential minimum. For this cladding configuration, the aluminum content of the barrier was gradually increased from 20% to 50% within a thickness of 10 nm. But as the grading forms a smooth transition, the carriers can be lost more easily at elevated temperatures because the phonon-carrier scattering and therefore the escape of carriers is not restricted to distinct phonon energies. Therefore the use of abrupt $\text{Al}_{0.50}\text{GaInP}$ claddings in combination with thin AlInP tunnel barriers (e) is recommended for high luminescence intensities at elevated temperatures. The temperature dependent PL intensity was fitted using a simple thermal activation model [6] to esti-

mate the activation energy E_A . In addition, time-resolved PL measurements were performed on the structures. As an example in the inset of Fig. 4 the transient of the PL maximum at 5 K can be seen for the structure with the abrupt cladding and AlInP tunnel barriers. The monoexponential behavior can be described using a model of the random initial occupation [7] to determine the decay times. The QDs display an approximately constant decay time (Fig. 4) up to 80 K with a linear increase at higher temperatures [8]. For elevated temperatures above 200 K the decay time

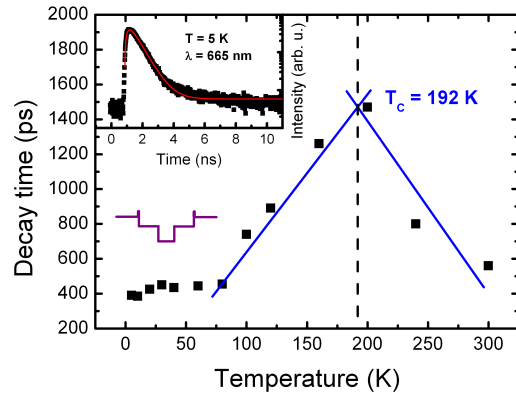


Figure 4 Experimental decay time and transient (inset) of InP-QDs in the abrupt cladding structure with tunnel barriers at the dot center wavelength ($\lambda = 665 \text{ nm}$) at 5 K. The inset shows the monoexponential decay, while the red curve is the fit derived from the model [7].

decreases due to excitonic dissociation to the barrier. We marked the intersection between the two fitted lines where the escape of the carriers into the barrier begins to dominate. This characteristic temperature T_C was estimated for all structures.

Table 1 summarizes the activation energies and the characteristic temperatures for the different structures under investigation. Within the error the thermal activation ener-

Table 1 Comparison of the thermal activation energy E_A and the characteristic temperature T_C of the various structures.

Structure	(a)	(b)	(c)	(d)	(e)
E_A (meV)	150	205	220	251	272
T_C (K)	150	140	150	160	192

gies can be increased from $E_A = 150 \text{ meV}$ for the reference structure to about 270 meV for the cladding structure with tunnel barriers. This increase can be attributed to the influence of the additional band offset of the barrier configurations. Furthermore, the characteristic temperatures significantly increase from 150 K up to 192 K. The reason for the low T_C -value of structure (b) is currently not known.

3.2 Micro-PL and autocorrelation measurements

In addition to the ensemble measurements, the zero-dimensionality of the dots was confirmed by performing μ -PL and second-order autocorrelation measurements on the samples. For single QD spectroscopy a 50 nm Cr layer was deposited and structured using a nanosphere lithography process (NSL) to produce holes with diameters of around 500 nm [9]. Fig. 5 displays the μ -PL spectra of the emission of a single QD with the reference Al_{0.20}GaInP-barrier, emitting at 1.916 eV at 4 K. The relatively large linewidth of 350 μ eV at 4 K is due to local carrier density fluctuations, also known as spectral diffusion, in vicinity of the QD [10].

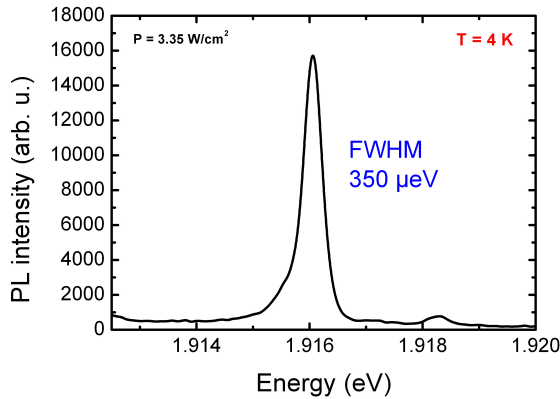


Figure 5 μ -PL measurement of a single InP-QD in an Al_{0.20}GaInP-barrier. For single-QD spectroscopy the sample was structured using a nanosphere lithography process.

The zero-dimensional nature of the emission source can be observed in the second-order autocorrelation measurement $g^2(\tau)$ of the QD emission line at 4 K.

The suppression of coincidence events at $\tau=0$ is equivalent to 11% of the calculated Poisson-normalized level (Fig. 6). This observation in turn indicates that the luminescence originates from a single InP-QD and that our structures are therefore capable of providing triggered single-photon emission.

4 Conclusion To summarize, in this work we have shown that the use of different barrier configurations does not affect the growth and therefore the optical characteristics of the investigated QDs. The temperature stability and the relative PL intensity can be strongly increased, using very simple barrier configurations (tunnel barriers) or more complex structures (combination of tunnel barriers with abrupt claddings). With the intensity from the latter increased by a factor of up to 20 at 240 K with respect to structures without barrier claddings. In addition, the estimated activation energy can be increased by increasing the total band offset of the cladding. Barrier claddings are therefore highly recommended for applications at elevated

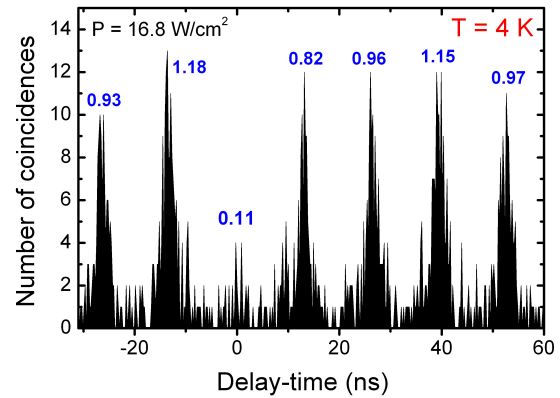


Figure 6 Autocorrelation measurement of the single-QD shown in Fig. 5 which displays a clear single-photon emission behavior at 4 K.

temperatures, such as p-i-n-LED and laser structures. In addition, μ -PL and autocorrelation experiments revealed the zero-dimensional nature of the QDs by clearly showing single-photon emission (antibunching) characteristics.

Acknowledgements Financial support by SFB TRR 21 and FOR 730 is gratefully acknowledged. We also would like to thank E. Kohler for technical assistance with the MOVPE system.

References

- [1] R. Roßbach, W.-M. Schulz, M. Reischle, G. J. Beirne, M. Jetter, and P. Michler, *Journal of Crystal Growth*, **298**, pp. 595-598, (2007).
- [2] Landolt Börnstein, *Numerical Data and Functional Relationship in Science and Technology* (ed. by K.-H. Hellwege, O. Madelung), Springer, (1982), edition 17.
- [3] W. Nolting, *Grundkurs Theor. Phys. 3, Elektrodynamik*, 8. Auflage, Springer-Verlag Berlin, (2007).
- [4] G. J. Beirne, M. Reischle, R. Roßbach, W.-M. Schulz, M. Jetter, J. Seebeck, P. Gartner, C. Gies, F. Jahnke, and P. Michler, *Phys. Rev. B* **75**, 195302 (2007).
- [5] R. Hanbury-Brown and R. Q. Twiss, *Nature (London)* **178**, 1447 (1956).
- [6] M. Sugisaki, Hong-Wen Ren, K. Nishi, and Y. Masumoto, *Jpn. J. Appl. Phys.*, vol. **41**, pp. 958-966, (2002).
- [7] K. Mukai, and M. Sugawara. *Self-assembled InGaAs/GaAs Quantum Dots*, vol 60 of *Semiconductors and Semimetals*, pp. 209, Academic Press, (1999).
- [8] D. S. Citrin, *Superlattices and Microstructures*, **13**:303, (1988).
- [9] U. Hakanson, J. Persson, F. Persson, H. Svensson, L. Montelius, and M. K. J. Johansson, *Nanotechnology* **14**, pp. 675, (2003).
- [10] F. Wang, A. Badolato, I. Wilson-Rae, P. M. Petroff, E. Hu, J. Urayama, and A. Imamoglu, *Appl. Phys. Lett.* **85**, 3423 (2004).